MEMS Micropump Characterization and Control Utilizing a Fibre Optic Interferometer.

Tom Tomac*
Katherine Wheeler, Anne Colonna[+], Paul R. Stoddart and Alex Mazzolini

Centre for Imaging and Applied Optics, School of Biophysical Sciences and Electrical Engineering, Swinburne University of Technology, PO Box 218, Hawthorn, Victoria 3122, Australia.
* Industrial Research Institute Swinburne
[+] Ecole Superieure d'Optique, Institut d'Optique , Centre Scientifique d'Orsay, France

ABSTRACT

In order to successfully integrate microdevices into functional systems, it is often important to address issues of real-time performance monitoring and control. The present study addresses some of these problems in the context of a piezoelectric-driven micropump. These devices are important for emerging areas of chemistry and medicine where reliable distribution of small quantities of fluid is required. A simple, low-cost, fibre optic interferometer has been used to measure the dynamic displacement of the micropump actuator surface. Measurements show significant differences in actuator velocity, displacement and settling time between different pumping media. In addition, transient underdamped vibration of the actuator surface was observed during the rapid excursion and recursion phases of the pump movement while pumping air. These non-contact measurements can be used to determine the open loop characteristics of the micropump and provide information for design improvement or failure analysis. However, the technique can also be used to provide continuous measurement for adaptive compensation, so that the pump performance criteria are always satisfied. To this end, an automated interference fringe counting algorithm has been developed, so that the steady-state parameters can be mapped into the closed-loop control elements in real time. The performance of this algorithm will be discussed, together with the implications for optimal control of the micropump and eventual integration of the interferometer and micropump systems.

Keywords: MEMS, optical fibre, interferometer, micropump, non-destructive testing, displacement measurement, condition monitoring, microsystem integration

1. INTRODUCTION

Microfluidic systems are emerging not necessarily from industrial demand but from the technologies that enable the fabrication of such microcomponents[1]. Increasingly, micropumps are used in biological, medical, chemical and pharmaceutical applications, where miniaturization reduces cost, improves accuracy, increases portability, and reduces the amount of biological or chemical samples required for analysis, whilst speeding up the measurement time. Reduction in size also implies reduction in quantity, so micro based processing plants are best suited for distributed processing of materials at the immediate point-of-use. In biomedical applications, an implantable micropump can be fabricated to accurately administer the amount of medicine required as the regulation of flow rates can be controlled precisely through integrated electronics.

Traditionally, feedback and control systems do not necessarily translate well into the microsystem domain. Numerous factors come into play in terms of characteristics and performance of such systems[2] and hence there is a need to investigate a range of problems in order to understand the methods and technologies that will be required to produce viable systems. In order to characterise the open and closed loop performance of a piezoelectric driven micropump, an accurate and reliable non-contact sensor should be employed. For the purpose of this study, a fibre optic interferometer was used in conjunction with an intelligent electronic microcircuit control system. Such a system forms the basis of an efficient and reliable adaptive microcontroller for the piezoelectric-driven micropump used in a real-time closed-loop application.

Smart Structures, Devices, and Systems, Erol C. Harvey, Derek Abbott, Vijay K. Varadan, Editors, Proceedings of SPIE Vol. 4935 (2002) © 2002 SPIE · 0277-786X/02/$15.00

Integration using the technologies, techniques and methods most suitable for the fabrication of microsystem components is also considered, with the objective of generating intellectual property for parameterisation of an adaptive and reliable piezoelectric driven micropump. This pump could be applied in a variety of microfluidic systems, particularly medical drug delivery, chemical and medical diagnostics, ink-jet printers, as well as any devices requiring transference of small quantities of liquids or gases. Numerous tests and procedures have been developed for the characterization of the dynamic performance of micropumps. The most effective measurements for the MEMS structures (which do not impede their performance) are achieved by the use of non-contact sensing techniques such as a fibre optic interferometer.

Typically, a microsystem will comprise of components categorised as microsensors or detectors (which detect any changes within the system environment), intelligent electronics (capable of making decisions based on the changes indicated by the sensors) and microactuators (capable of altering the system environment according to the directives from the intelligent electronics). In order to identify potential causes of failure in both electrical and mechanical elements of a microstructure, it is imperative that a suitable measuring system is used that does not perturb pump performance.

This paper describes the use of a non-contact fibre optic based interferometer for measuring the externally-driven dynamic displacement of a micropump micro electro mechanical system (MEMS). This approach ensures that the optimum displacement of the piezoelectric actuator membrane is maintained for any given gas or liquid being pumped through the micropump's valves and chambers.

2. METHODS AND PROCEDURES

This research investigates the characterization of a micropump using a fibre optic interferometer as a sensor for the measurement of the piezoelectric membrane displacement. A study of the dynamic actuating properties such as actuating currents, frequencies and duty cycles has been undertaken in order to optimise the actuating performance of the micropump in a microfluidic system.

The detectors and actuators exist as separate units for the purpose of this study, but ultimately the preferred option is to integrate them into a single self-contained unit. This paper examines the integration processes from the aspect of miniaturization, performance optimisation, monitoring and controlling methods, which can be synthesized to form an efficient and reliable closed loop system. The integrated system can be interfaced to a computer by using single or multiple ports that allow transmission of information between the controller, detector and the computer. In addition, direct monitoring of the drivers associated with controlling the microactuators (which is based on the decision making intelligent electronics) is also possible via optically isolated ports.

It is envisaged that the outcome of this study will provide the basis for the design and development of a non-contact, high–bandwidth, in-system interferometer. This will be used as the sensor for the dynamic measurement of a MEMS micropump, interfaced with hybrid or polymer-infused electronic components capable of controlling actuating voltages, frequency and duty cycles in a closed loop environment. Closed loop actuators are ideal for applications requiring high linearity, long-term position stability, repeatability and accuracy and, when used in conjunction with a position measuring sensor and microelectronic circuits, form an intelligent and reliable microfluidic control system.

2.1 Micropump

This project employs an IMM self-priming membrane micropump[3] with physical dimensions of 13x12x3 mm^3, 250 µl/min flow rate, 400 volt piezoelectric actuator drive, and a 5 ms pulse of varying frequency (Figure 2-1).

The micropump operation is dependent on the displacement of a membrane actuator driven by a piezoelectric plate[4] which is energized by the positive-edge of a square wave pulse (400V peak). The upward deflection of the membrane actuator has the effect of decreasing the chamber pressure and increasing the volume, forcing the liquid or gas medium into the main chamber. During the downward deflection of the piezoelectric membrane actuator (caused by a negative

edge of the pulse) the pressure increases and the volume decreases, forcing the liquid or gas in the main chamber out through the outlet valve. The piezoelectric membrane actuator driver must be capable of supplying a square wave of varying actuating voltage, duty cycles and frequency in order to characterize the effect on the displacement while pumping different media.

2.2 Fibre optic interferometer

The displacement of the micropump membrane actuator is measured using a fibre optic interferometer (Figure 2-1) in a modified Mach-Zehnder configuration using a 630 nm single mode fibre (SM), two 50/50 fibre optic bidirectional couplers, and a 1.2 mW (632.8 nm) Helium Neon (HeNe) Melles Griot laser source.

The fibre optic interferometer is positioned such that the signal beam is focused at an optimum displacement point on the piezoelectric actuator (typically the centre). The light beam from the HeNe laser is passed through a 3dB fused fibre optic directional coupler (DC1, 2 x 2 splitter), splitting it into two beams of equal intensity. The signal arm beam is then expanded by a collimating lens and then focused at the surface of the piezoelectric actuator whilst in a non-actuating state. A proportion of the beam focused at the actuator surface is reflected back into the signal arm and then combined with the reference beam when passed through the second fibre optic directional coupler (DC2). The outputs from DC2 are 180º out of phase and are sensed by photodetectors, which convert the respective intensities into electrical signals. Any phase modulation of the signal and reference light beams will produce interference fringe patterns proportional to the displacement range of the actuator. An instrumentation amplifier is used to calculate the differential of the photodetector outputs as intensity modulations over a number of cycles for the generated sinusoid. A predetermined trigger point starts the fringe counting over the actuator displacement range and by interpolation of the generated sinusoid a precise measurement of the actuator displacement is then calculated. A fibre wound piezoelectric cylinder is used in the reference arm to lock the interferometer at the quadrature point to accurately control the low frequency phase shifts between the two arms (signal and reference) caused by temperature drifts.

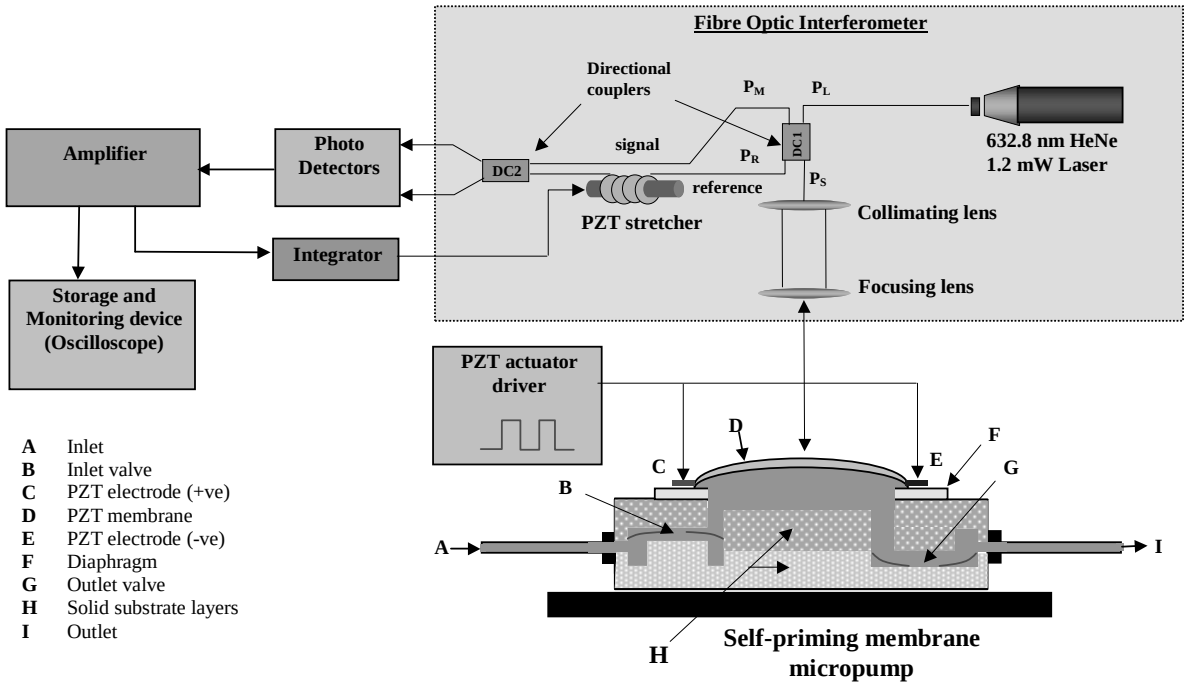

Figure 2-1 Open loop fibre optic interferometer

2.3 Intensity modulation fringe to actuator displacement conversion technique

The sampled modulation fringes (Figure 2-2) are analysed using a discrete form of an adaptive filter. The local maxima and minima are identified and the frequency extrapolated then converted into voltage amplitudes by differentiating between the valid maximum points. The higher the frequency, the steeper the displacement slope that occurs during the rapid excursion and recursion phases of the piezoelectric actuator (see Figure 3-2). Electrical and mechanical noise is filtered out using linear interpolation. The signal-processing algorithm is applied using hardware high-speed techniques. The first stage of the process examines the zero-crossing points that may be shifted according to the trigger requirement. Low pass filters prior to buffer storage remove the drifts associated with the instability due to temperature and amplifier offsets during real-time operation of the system. The zero crossing on a rising edge of the signal is sampled and minimum and maximum points are extracted. This is done over the period determined by the PZT driver rising edge output, which is used as reference for the displacement differential. The differentiation of minimum and maximum fringe peaks identifies the frequency at each zero crossing and serves as reference for the displacement counting technique.

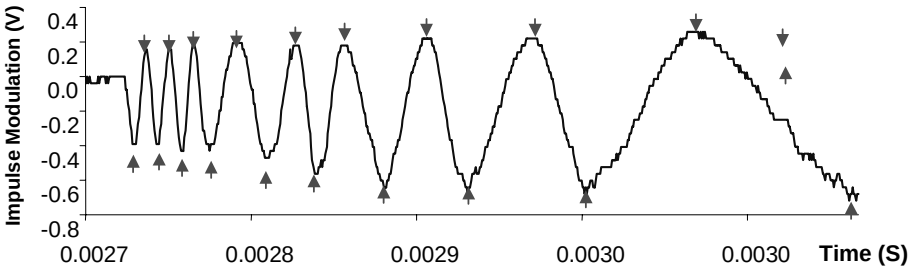

Figure 2-2 Fringe processing

2.4 Micropump closed loop considerations

The micropump characterisation takes into account the structural, mechanical, chemical and electrical parameters that are susceptible to steady-state variations attributable to electrical noise, temperature, vibrations, inductance, capacitance and chemical reactions. In a closed loop control system the performance is measured by its steady-state error, gain and phase margins, which are essentially the criteria for optimality. The performance and reliability of a micropump is only as good as its feedback compensation, which maximises or minimises the performance index that is unknown until the completion of the optimising process. Figure 2-3 illustrates a simple adaptive control system for a micropump with several parameters that are continuously measured and then compensated so that the system performance criteria are always satisfied.

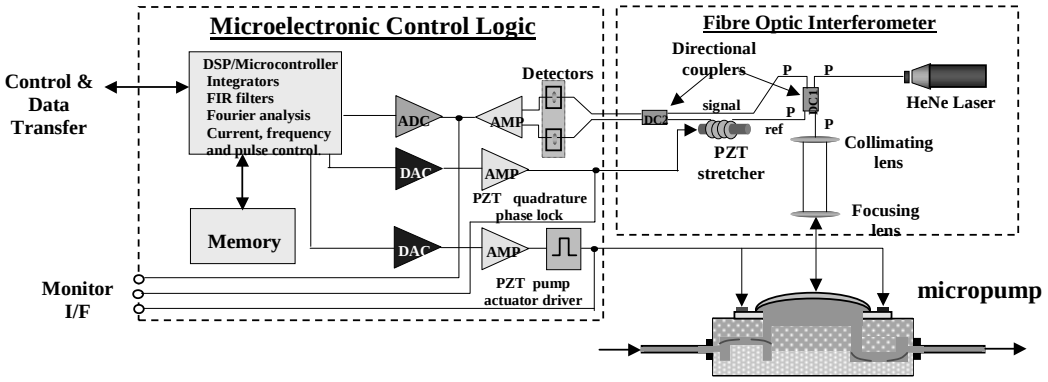

Figure 2-3 Micropump feedback control system

When considering a closed loop system for a micropump it is imperative that the chosen design parameters closely match the ideal responses to minimise the performance index or the error between the actual and ideal response.

2.4.1 Closed loop controlling elements and parameters

The fibre optic interferometer requires feedback compensation for the low-drift induced phase changes in order to precisely lock the interferometer at the quadrature point[5]. The compensation factor can be expressed as a function of the error where the controlling element is a phase shifter (Figure 2-4).

P_I=Optical Interference
P_M=Optical Displacement Signal
P_R=Optical Reference Signal
ϕ=Phase
γ=Interference Error

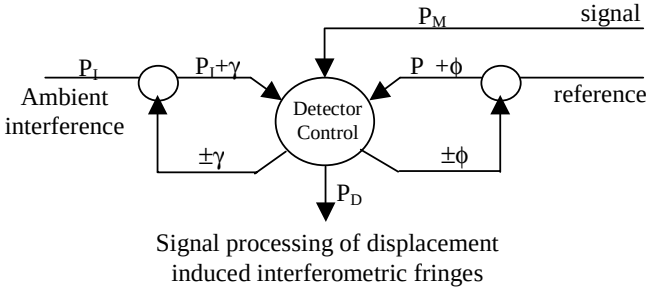

Figure 2-4 Interferometer closed-loop feedback path

Equally, ambient interference at the input to the photodetector may be sufficiently high to induce a fringe pattern distortion, which needs to be minimized or eliminated altogether as it may produce additional patterns that would be processed as valid fringes and therefore producing erroneous results. The micropump piezoelectric actuator controlling elements are amplifiers, frequency generators, phase shifters, noise cancellers, pulse-width modulators and filters, each of which is capable of affecting the output of the actuator. The control logic is contained in microelectronic circuits capable of manipulating the parameters of the controlling elements described in the previous two sections. The intelligence for the control logic is implemented via a digital signal processor (DSP). Additional sensors (such as thermistors, accelerometers, piezoresistors, capacitive or flow rate sensors) may also be included in the closed-loop system, keeping in mind that they should not impede the overall system performance.

Figure 2-5 shows a basic block diagram of an adaptive control system that can be used to optimise the performance of a micropump. All of the parameters which are known to vary with time are continuously measured at the input *c(t)* and output *d(t)* of the "Piezoelectric Actuator". These parameters are processed in the "Parameter Optimisation" block in order to identify which parameters require adjustment in the "Control Elements" block to satisfy system specifications. Included in the "Parameter Optimisation" block are the fibre optic interferometer parameters which are not shown as a separate feedback path.

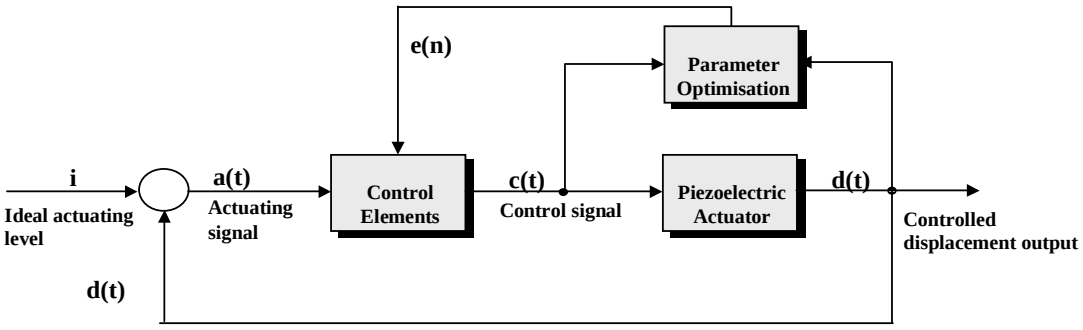

Figure 2-5 Adaptive micropump control system

Most of the signal processing is included in the "Parameter Optimisation" block, passing only the error signal *e(t)* to the "Control Elements" block where the appropriate coefficients are modified and sent to the "Piezoelectric Actuator" block.

2.4.2 Detection electronics

The detection electronics consists of a suitable photodetector, instrumentation amplifier, and an analog to digital converter. Each photodetector uses a silicon photodiode which is sensitive to a wavelength of 632.8 nm. The photodiode acts as a light-controlled current source operating in its linear range, and uses an amplifier where the current is converted to voltage proportional to the level of illumination. UDT Sensors manufacture the photodiode used (which have a sensitivity of 0.37 A/W at 632.8 nm and linear output current of up to 100 μA in photovoltaic mode). The photodiode has an active area of 0.77 mm^2, capacitance of 4.5 pF at 5V reverse bias, shunt resistance of 10^{11} ohm, and a rise-time of 1.0 ns.

The photodetector amplifier module (PAM) is made up of a number of amplifier stages, each biased for optimum performance based on the characteristics of the individual operational amplifiers used. In order to minimize the effect of input bias currents and allow for detection of low photocurrents, wideband JFET operational amplifiers were selected. Additionally, in order to maximize the 3dB bandwidth, the JFET-input operational amplifier should have a high unity gain-bandwidth product, and a low input capacitance. The bandwidth for the preamplifier f_{bw} is given by the following equation:

$$f_{bw} = \sqrt{\frac{f_u}{2\pi R_f C_x}}, \qquad (1)$$

(where f_u is the unity gain bandwidth product, $C_x = C_j + C_{in}$, C_j and C_{in} are the junction and input capacitance respectively, and R_f is the feedback resistance).

2.4.3 Process and control electronics

The central processing and control module (CPCM) interfaces with a number of peripherals such as the photodetector module, memory expansion card and the piezoelectric actuator driver. Signal processing is achieved by using a fast hardware algorithm that is dynamically configurable during the real time operation of the system. Data transfer is achieved via serial communication ports and the configuration of the hardware is made possible through the In-System-Programmable (ISP) port during power-up using a serial programmable read only memory (PROM) device. The digital signal processing functions, such as finite impulse response filters (FIRs), Fourier analysis, convolution, differentiation, integration averaging, phase shifting, and signal smoothing are implemented in a complex programmable logic device (CPLD) during real time operation. Sampled data is stored after processing for each of the amplitude-triggered cycles and then compared with the previous sample to determine the error coefficient required to control the piezoelectric actuator elements in the next sample. This process is referred to as an adaptive control of the system since it continuously measures the input and output of the micropump parameters. The lead compensation function can then be modified by the output of the elements to satisfy the open-loop system specifications.

The experimental results for this research were obtained using both the PAM and CPCM modules, developed using standard printed circuit board (PCB) fabrication processes and fitted with application specific integrated circuits based on preliminary specifications and requirements for micropump characterisation. First, data is accumulated at a rate of 1 Mbps and stored in an array of 100 samples which allows for progressive averaging and filtering over that period. The samples are then differentiated for maximum and minimum turning points and relative phase angles. The resulting slopes are analysed for amplitude reference crossings with peak amplitudes extracted and digitised, generating a clock with a frequency proportional to the captured interferometric fringes. Sampling is continuous and displacement is calculated over a complete actuating cycle having an "ON" period of T = 5 ms and "OFF" period dependent on the pumping frequency. Since the ratio of the duty cycle is variable, the elements of the lead compensator (closed loop feedback parameter) can be modified to satisfy system specifications based on the adaptive control requirements.

In order to satisfy control loop requirements for a steady state response, the sum of integrals, or the area of the displacement is correlated with the preceding samples and the variations are used as error coefficients for adjustments within the lead compensation elements of the system. The area integral for the displacement can be expressed as:

$$\text{Area} = \sum_{N} \int_{t_{n-1}}^{t_n} u\,dt \tag{2}$$

where N is the total number of samples, u is the displacement function and $u = f(t)$ between the t axis and the ordinates at t_{n-1} and t_n (which are the subset samples).

Using digital interpolation, the area integral can be expressed as:

$$f_n(t) = u_n\left(t_{n+1} - t_n\right) + \frac{\left(u_{n+1} - u_n\right)\left(t_{n+1} - t_n\right)}{2}. \tag{3}$$

2.4.4 Proposed system integration

A complete and fully integrated micropump feedback closed-loop system will be developed using the preliminary investigation (experimentation, methodology and analysis) outlined by this study. The interferometer section could be constructed using inorganic polymer glass, miniaturised using specialised techniques, not unlike those used for making semiconductors, and linked using fibre optic waveguides designed to meet the required specifications. The optics could be sealed and isolated in an epoxy resin with a high temperature coefficient to minimise low frequency drifts. There are a number of manufacturers of polymer-based optics willing to custom make the required fibre channels, splitters, mirrors and collimating/focusing lens that may be used to form an optical circuit to the specification required for this interferometer.

The structure of the microelectronic circuit is very complicated and difficult to manufacture because of its three-dimensional composition. It is made up of many layers, each of which has its own unique pattern associated with a particular type of architectural requirement.

The sensing electronics (photodetectors) could be included as a separate layer, based on hybrid technology and microelectronic fabrication techniques such as lithography. These are linked to the controlling electronics through a number of optically isolated channels to minimise noise. The sensing, controlling and actuating elements are split across three different planes, each configured as a layer encapsulated within its own epoxy resin. The actuating electronics must be isolated from other layers as the PZT driver produces pulses of up to 400V dc. A suitable power cell is sealed and located away from the high voltage inverter transformer and is only enabled during pumping.

3. RESULTS AND DISCUSSIONS

The following results show the relationship between the impulse modulation fringes and the piezoelectric actuator displacement as measured with the fibre optic interferometer. Figure 3-1 illustrates how the intensity modulation fringes amplitude and frequency components depend upon the actuator peak driving voltage and its rate of change. The steeper the slope (rate of change) of the actuator driving voltage, the higher the frequency of the intensity modulation fringes (and the lower their amplitude due to bandwidth limitations governed by Eq. 1).

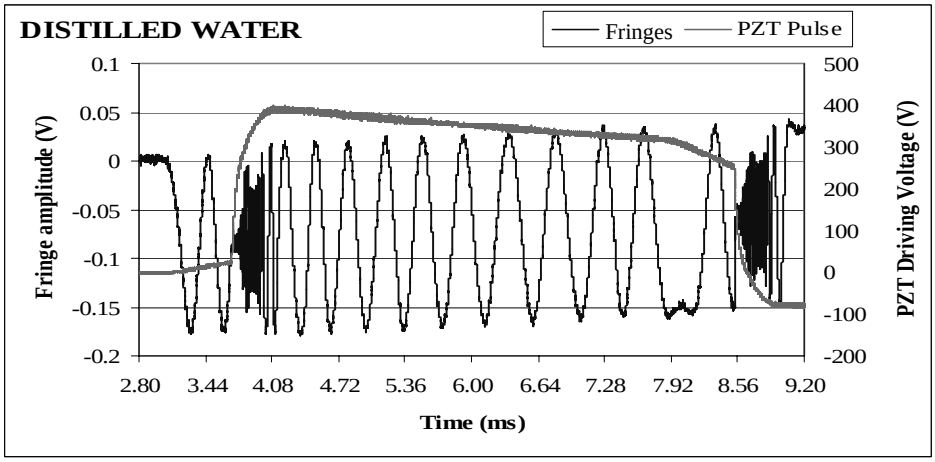

Figure 3-1 Piezoelectric actuator pulse and displacement elicited modulation fringes

Figure 3-2 represents a positive excitation fringe pattern for the displacement of the micropump diaphragm when pumping water. Note the dc or low frequency preceding the high frequency fringe sinusoids that is used as a signature for the beginning of the diaphragm displacement; it has a distinct and incomplete cycle transient function, indicating a sudden change in the diaphragm position.

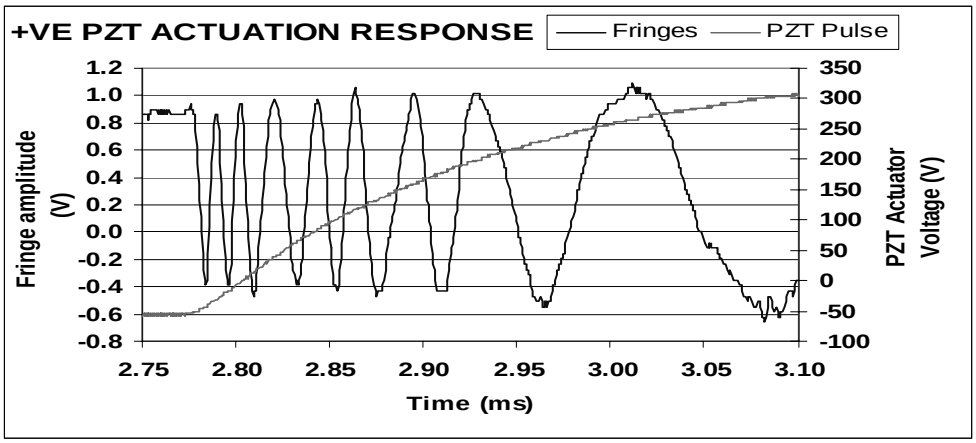

Figure 3-2 Positive PZT actuation and the interferometric fringe response

By differentiating across the generated fringes and extrapolating the maximum and minimum points, we can plot the rate of increase dV with respect to t, where dV/dt is the differential coefficient of the actuator displacement amplitude V with respect to t. The turning points are determined using the $dV/dt = 0 = tan\theta$, and the subsequent frequency interpolated from the distribution of minimum and maximum peaks. The displacement of the diaphragm is measured by the number of fringes that are proportional to the wavelength of the source. During the positive transition of the applied PZT potential, a sudden change in frequency is used as a trigger point for the initialisation of the displacement signal-processing algorithm (Figure 3-3). Data is averaged over a number of samples to filter out the high frequency noise. The averaging distribution factor is determined from the amplitude of noise carried by the fringe sinusoids. This is a calibrated adaptive function that can vary within a predetermined range of parameterised coefficients.

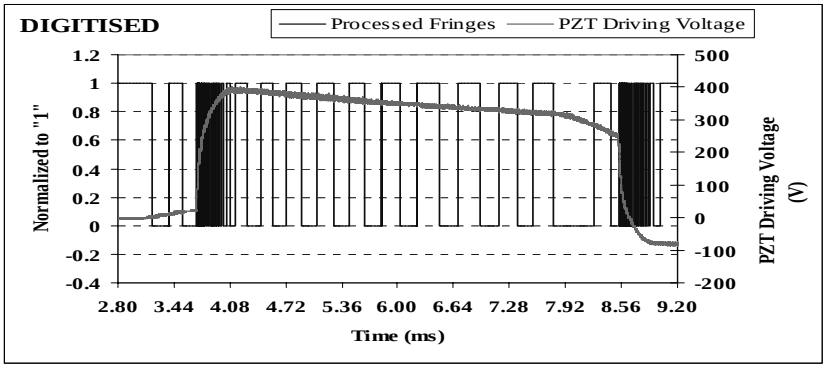

Figure 3-3 Digitised fringe modulations using the DSP algorithm

It has been found that the elements controlling the actuation slope parameters must be dynamically configurable in order to limit the bandwidth within acceptable boundaries for optimum amplifier performance. The boundary limitations are pre-programmed into the coefficient tables and are used adaptively for characterisation of the displacement under different pumping fluids of varying viscosity.

The shape in Figure 3-4 illustrates the effect of free vibration ringing, which may be attributed to the rapid excursions of the membrane due to decreased resistance whilst pumping air. The increased flow resistance for water as compared to air may be the reason for the obvious reduction in the amplitude of the actuator membrane displacement. In addition, a greater variation in actuator displacement is observed when pumping water rather than air (Figure 3-5). This displacement variability, which occurs with identical pump cycles and piezoelectric actuator driving voltage over the acquired sample periods, might be associated with flow rate instability caused by membrane valves[5].

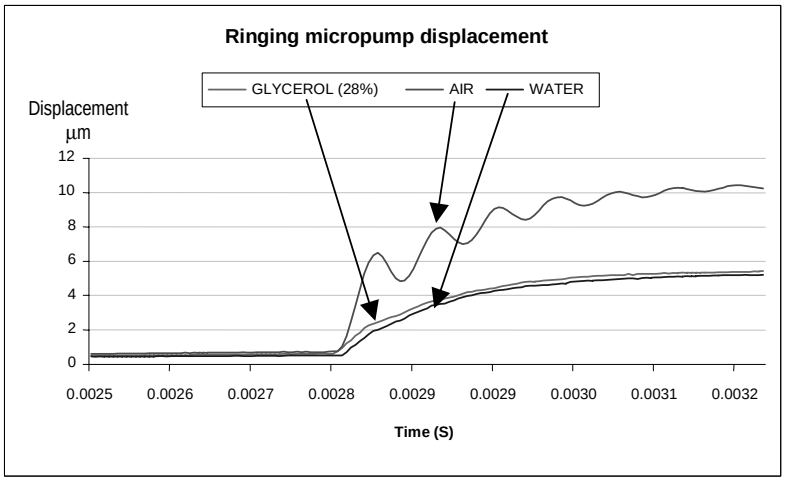

Figure 3-4 Ringing section of micropump displacement[5]

The pumping medium viscosity and density determines the volume of material that will flow through the pump chamber during each pump cycle. This is expected during the open loop operation since piezoelectric actuators exhibit hysteresis and creep behaviour (like any other open loop systems) and when loaded, their dynamic characteristics may be altered. One way of maintaining long-term position stability, repeatability and accuracy is to include feedback control for the piezoelectric actuator.

Figure 3-5 shows three displacement samples for water taken 32 periods apart using the same experimental set-up. It can be seen that the waveforms do not necessarily follow exactly the same path, and the variations might be attributable to flow rate instabilities. Such instabilities may be associated with complex membrane valve behaviour in both the forward and reverse flow directions.

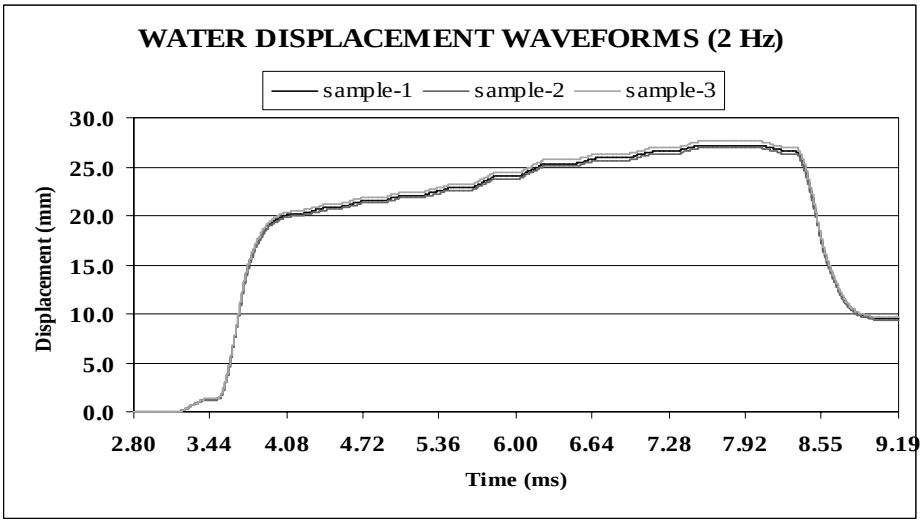

Figure 3-5 Three samples of water displacement using identical experimental procedures taken 32 cycles apart

Additionally, localized variations in membrane stiffness, thickness & mass, bonding of the metal diaphragm along with localized variations in the piezoelectric driver elements might also cause small changes in the open loop steady state coefficients. There are many elements that might contribute to the variations in the membrane displacement, which only demonstrates the need for a reliable and efficient closed loop adaptive system.

When pumping water with 60% glycerol added, the displacement is significantly reduced (Figure 3-6) due to the increase in the viscosity. It was shown that for the same experimental conditions the volume of fluid flowing through the micropump chamber during each pump cycle is dependent on the fluids density and viscosity. For an excitation frequency of 2 Hz and a duty cycle of 1% "ON" (5 ms) to 99% "OFF" (495 ms), the maximum actuator displacement was 27.2 μm when pumping water, 21.9 μm when pumping water with 28% glycerol added to it, and 15.2 μm when pumped with water with 60% glycerol added to it.

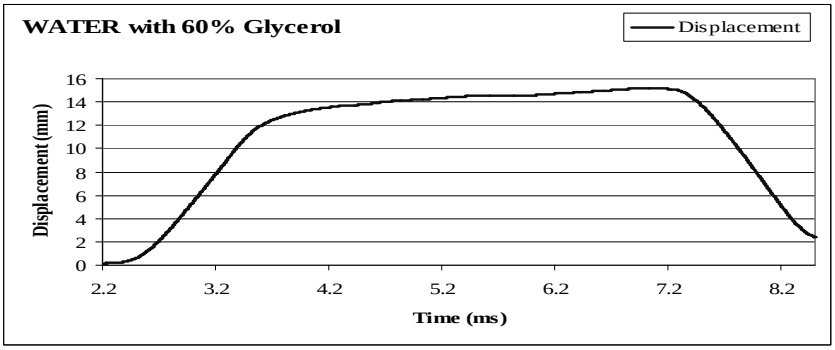

Figure 3-6 Displacement when pumping water with 60% glycerol

It was also shown that the pulse repetition frequency driving the piezoelectric actuator has the effect of linearly varying the amplitude of the membrane displacement. A number of pumping frequencies were plotted against the membrane displacement, which showed a decrease in amplitude with increase in frequency (Figure 3-7).

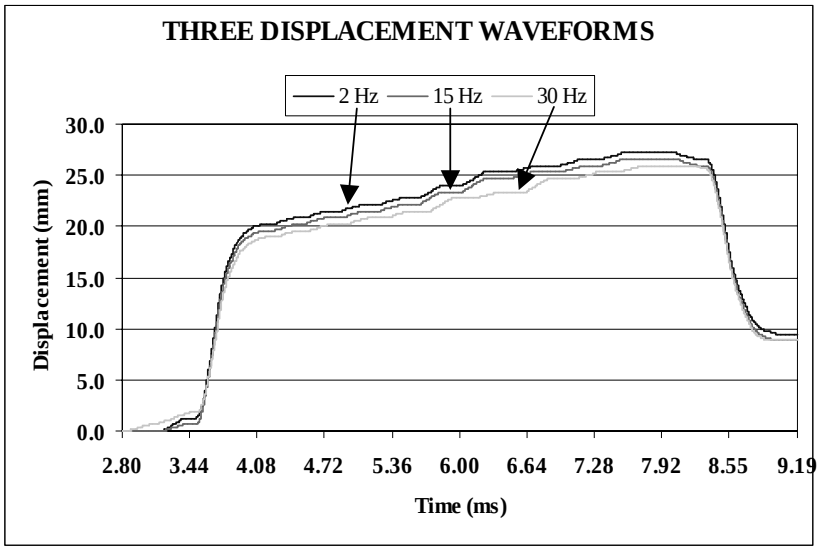

Figure 3-7 Three displacement waveforms for water at different pumping frequencies

Figure 3-8 shows the area of displacement for the period of each sample where the displacement decreases as the frequency of actuation increases (Eq. 2 & Eq. 3). This is useful since the variations in frequency can control the feedback loop elements that compensate for the variations in the steady state of the open loop system.

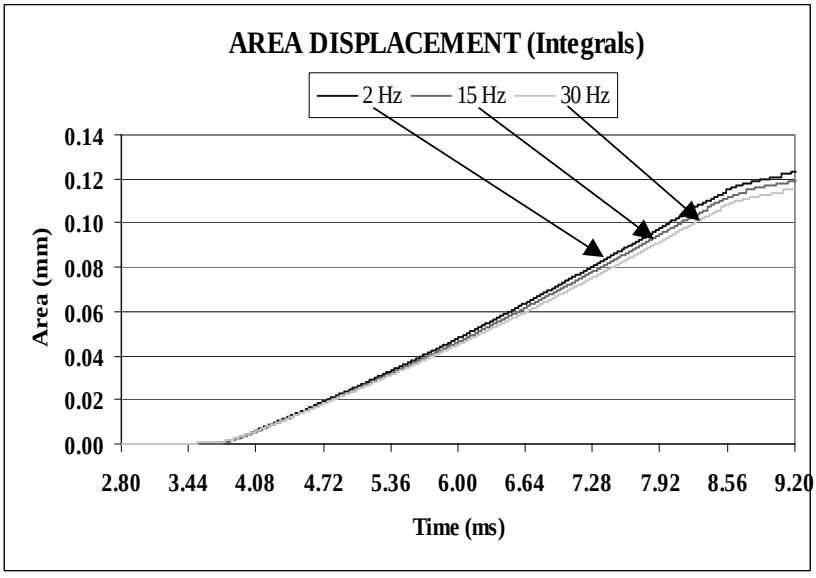

Figure 3-8 Displacement area for the samples taken at three frequencies

4. CONCLUSION

Design and test techniques were applied to a simple MEMS micropump system with the objective of identifying and parameterising the steady-state dynamic variables during the displacement measurement of the piezoelectric actuator, using a non-contact fibre optic interferometer. The parameterised evoked potentials (elicited by the fibre optic interferometer) were accumulated and processed to identify control elements that may be applied in an adaptive closed-loop environment. It was shown that the displacement of the piezoelectric actuator is dependent upon the viscosity and density of the pumping medium, as well as the peak PZT driving voltage, its rate of change and its frequency. Fully functional and experimentally optimised electronic modules have been developed which incorporate high bandwidth photodetector amplifiers, high speed analog to digital converters, a digital signal processing unit and a high voltage inverter for feedback control of the piezoelectric membrane actuator. It is conceivable that all of the digital signal processing elements may be implemented in one single complex programmable logic device (CPLD). This would allow for dynamic re-programmability implementation on demand, which would be beneficial for applications requiring control logic (functional) changes without having to modify the physical layout or structure of the system. It was also demonstrated that it is possible to produce an adaptive closed-loop system model based on the characterisation of a micropump using a fibre optic interferometer.

REFERENCES

1. F. Forster, R. Bardell, M. Afromowitz, and N. Sharma, "Design, fabrication and testing of fixed-valve micropumps," *Proceedings of the ASME Fluids Engineering Division. FED-VOL.* **234**, pp. 39-44, IMECE 1995.
2. T. Gerlach and H. Wurmus, "Working Principle and Performance of the Dynamic Micropump," *Sensors Actuators A* **50**, pp. 135-140, 1995.
3. *µl-flows and dosages: The IMM-Micropump* data sheet IMM 3/1998 E 01.
4. C.J. Morris and F.K. Forster, "Optimization of a circular piezoelectric bimorph for a micropump driver," *J. Micromech. Microeng.* **10**, pp. 459-465, 2000.
5. C. Davis, D.J. Booth, E. Harvey, P. Cadusch, A. Mazzolini, and S. Askraba, "Dynamic measurements of a micropump using a fibre optic based interferometer," in *Proc. of the EOS/SPIE Symposium on Applied Photonics*, ed. by R.R. Syms, SPIE Vol. 4075 Micro-Opto-Electro-Mechanical Systems, pp. 101-108, Glasgow, 2000.